An experimental investigation on synthesis of nanocrystalline nickels by pulsed current electrodeposition has been carried out in an additive-free Watts bath employing nickel-sulphate solution with similar nickel ion concentrations. Aluminum was used as a substrate. It demonstrated the advantage of easier removal process of electrodeposited nanocrystalline nickel from its substrate. Whereas the use of high-purity nickel anode was intended to replace nickel ions, which decreased during electrodeposition. Different peak current densities of 450, 750 and 1000 mA/cm^2 were applied. A pulsed current was set at a similar pulse pattern of on-time and off-time of 1 ms and 9 ms respectively. The shorter on-time demonstrated the ability to limit ion deposition, which was related to the formation of finer grains. The off-time arrangement was targeted to ensure that the ion mobility had completely stopped. Higher current density demonstrated a dominant impact on deposits, generating a higher nucleation rate that is related to depositing nanocrystalline nickel. A peak current density of 1000 mA/cm^2 produced grain sizes in the nanoscale regime.

Without any additional additive, nanocrystalline nickel was successfully yielded. Investigation of grain size obtained from the 1000 mA/cm^2 has been conducted by extracting full width at half maximum peak intensity (FWHM) revealed from X-ray diffraction (XRD) and Transmission Electron Microscopy (TEM) exhibited consistent results of 22 nm and 25.4±3.4 nm, respectively. It is also evidence of the significant role of pulsed current density. In inclusion, nanocrystalline nickel can be synthesized in an electrodeposition bath without any addition of additives

Keywords: nanocrystalline, nickel, nanoscale, electrodeposition, additive, pulsed current, nucleation rate, pyramidal, FWHM

UDC 502

DOI: 10.15587/1729-4061.2024.298302

SYNTHESIS OF NANOCRYSTALLINE NICKEL VIA PULSED CURRENT ELECTRODEPOSITION IN ADDITIVE-FREE DEPOSITION BATH AND COMPARISON OF NANOSCALE CHARACTERIZATION

Rahmad Imbang Tritjahjono
Doctorate, Associate Professor
Department of Mechanical Engineering
Politeknik Negeri Bandung
Gegerkalong Hilir str., Ciwaruga, Bandung, Indonesia, 40558
E-mail: r.imbang@polban.ac.id

Received date 29.11.2023
Accepted date 06.02.2024
Published date 28.02.2024

How to Cite: *Tritjahjono, R. I. (2024). Synthesis of nanocrystalline nickel via pulsed current electrodeposition in additive-free deposition bath and comparison of nanoscale characterization. Eastern-European Journal of Enterprise Technologies, 1 (12 (127)), 13–19. doi: https://doi.org/10.15587/1729-4061.2024.298302*

1. Introduction

Extensive research in synthesis of nanocrystalline metals has been reported. Additives, for instance, saccharine ($C_7H_4NO_3S$) were employed. It revealed unexpected elements in the deposit such as Sulfur in the deposit. In mechanical uses, a hard coating is needed to improve the wear resistance. The effect of Sulfur in the deposit has not been discussed extensively. High purity nanocrystalline Nickel was needed.

The research on synthesis of nanocrystalline nickel should be conducted in an electrodeposition bath without any additional additives. Scrutinizing grain size was the most important step to ensure the expected result. On one hand, by using TEM, grain size characterization can be done accurately, in the other hand it needs great effort for sample preparation. Hence, for comparison purposes, the determining of average grain size was also conducted by employing the Scherrer equation which is based on the FWHM extracted from its X-ray diffraction. чTherefore, research on synthesis of nanocrystalline nickel in an additive free deposition bath and its characterization were relevant.

2. Literature review and problem statement

Extensive research has been conducted over the past two decades regarding the synthesis of nanostructured coatings in anticipation of their high demand in the industrial sector [1, 2]. Among these materials, nickel stands out due to its excellent properties in terms of wear and corrosion resistance. The scientific reports published the findings increasing the microhardness of nanocrystalline nickel [3]. A review of the purpose of nickel was confirmed as an extraordinary element for increasing the ability to increase corrosion resistance. It was also suggested as an important element for improving mechanical behaviour [4]. The wear problems experienced in tools were suggested to be able their lifetime by nickel as one of the important alloying elements [5]. In addition, a significant finding concluded the improvement of wear resistance obtained from the coating of Ni-CeO_2 nanoparticles onto the surface of anodic titanium oxide (ATO) surface with nanoporous structure [6]. The paper [7] presents the result of the effectiveness of electrodeposition of nanocrystalline Ni-WO_3. The two major sources of Ni and WO_3 including $Ni(SO_3NH_2)2{\cdot}4H_2O$ and $Na_2WO_4{\cdot}2H_2O$ respectively were applied. Formation of

$Ni\text{-}WO_3$ involved inverse hydrolysis. However, the potential decrease of both ion concentrations in the electrolyte had not been reported.

In terms of corrosion resistance, as concluded in the paper [8], nanocrystalline Ni has been reported to be able to improve the corrosion resistance of a magnesium alloy. Although it could be deposited by electroless plating, direct current electroplating was demonstrated to be able to enhance the results. This was strongly attributed to the effectiveness of the deposition that yielded a pore free deposit. On the other hand, the electroless deposition successfully deposited Ni-P alloy onto a nanoporous substrate of anodic titanium oxide (ATO). Enhancement interface bounding was merely improved by the existence of nanoporous substrate which was prepared by direct current anodization [9]. Other methods such as hot dip can be applied for metal coating. The microstructure of deposited metal was accomplished by solidification of molten metal coated onto a metal surface. So far, the coarse gain sizes have been observed [10]. In addition, there have been no discoveries that report the existence of additives to stop grain growth during solidification period. An outstanding coating process conducted by laser cladding exhibited the appearance of porosity of deposit [11]. Additionally, the success of the thermal sprayed method was reported excellent SEM images which exhibit the presence of microstructures. Further, the cost effectiveness still has to be considered [12].

In synthesis of $Ni\text{-}Al_2O_3$ nanocomposite coatings using electrodeposition, the physical properties such as grain size, hardness, and microstructure are affected by the chemistry of bath, acidity, and temperature [13]. Also, DC and pulsed current can be used to control the properties of electrodeposited nickel.

Investigation of the effect of several parameters on the formation of nanocrystalline nickel has been conducted with deep attention on the elemental mapping. Deep scrutinization of the role of additive was repotted, in which sulfur was found as an impurity that resides in between Ni structures. The sulfur was believed to come from a saccharine additive, which assisted in limiting nickel deposit growth [14]. Unfortunately, C and O were unrevealed clearly. In related study, nanocrystalline of medium entropy alloy of FeCoNi were produced by electrodeposition processes in aqueous solution containing boric acid, hydroxylammonium chloride, saccharine sodium dihydrate, sodium dodecyl sulfate, nickel(II) sulfamate tetrahydrate, cobalt(II)sulfate hyptahydrate and iron(II) sulfate hyptahydrate. Nanocrystalline FeCoNi with grain size of 10 nm were obtained. Enhanced mechanical properties of tensile strength, hardness were reported [15].

Studies examined the additive free electrodeposition in different deposition baths containing nickel sulfate (NS) and nickel sulfamate (NSA). Nanocrystalline Ni-B were reported to have grain size ranging from 10 to 25 nm were measured by utilizing Scharrer formula [16]. In addition, an average grain size of 30 nm or less was observed at current densities of 50 mA/cm^2 or higher [17]. A similar experiment utilizing rotating cylindrical electrodes and the same additives, nanocrystalline nickel was deposited at a rotation speed of 500 rpm and a current density of $2A/dm^2$ [18]. The range of grain sizes varied from 8 to 25 nm, with an average grain size of 13.5 nm. Moreover, a decrease in microhardness from approximately 600 to 400 HV was also observed over a current density range of 2.5 to 22.5 A/dm^2.

In terms of the structure and hardness of nanocomposite coating, deep focus was examined to determine the effects of the duty cycle on its properties. Results revealed that an increase in the duty cycle from 6 % to 17 % led to higher hardness, while nanometer-sized particles were observed when the duty cycle was increased from 6 % to 9 %. In a related study, the impact of the duty cycle during pulse electrodeposition on the properties of Ni-SiC was investigated [19]. The duty cycle between 20 %, 40 %, and 80 %, with the frequency of 10, 25, and 50 Hz, as well as the current density of 40 mA/cm^2 were varied. The study demonstrated that finer grains were obtained at a frequency of 25 Hz. The highest microhardness and lowest wear weight loss were found at a duty cycle of 20 % and pulse frequency of 50 Hz, which produced the highest impedance of the nanocomposite, indicating the highest level of corrosion resistance.

Despite previous studies on electrodeposition of nanocrystalline nickel, only a few have discussed the effect of nickel ion concentration on grain size distribution. To address this gap, this study aimed to investigate the effects of current density on the formation of nanocrystalline nickel by using electrodeposition in additive-free baths. Various analyses, including SEM, TEM, and XRD were employed in order to examine the results of experiments conducted with different peak current densities, duty cycles, and nickel ion concentrations.

3. The aim and objectives of the study

The aim of the study is to ensure that nanocrystalline nickel can be synthesized in a deposition bath in absence of additives.

To achieve this aim, the following objectives are accomplished:

– to synthesis nanocrystalline nickel in an additive free deposition bath;

– to conduct and make comparison of nanoscale characterization through recommended methods.

4. Materials and methods of research

4. 1. Synthesis of nanocrystalline

An experimental study was conducted to synthesize nanocrystalline nickel through pulsed current electrodeposition in nickel-sulfate solution using Watts bath. The electrodes were set parallel with the distance of 5 cm. Similar to [20], this study was set at deposition baths containing of $NiSO_4{\cdot}6H_2O$, $NiCl_2{\cdot}6H_2O$, H_3BO_3, and sodium lauryl sulfate (SLS), while the temperature was maintained at 60 °C and 65 °C. The electrolyte composition, peak current densities, as well as pulse cycle are shown in Table 1. In addition, the sodium lauryl sulfate was added to increase the ionic mobilities toward the cathode [21].

As shown in Fig. 1, experimental apparatus was composed of a nickel sheet with 99.95 % purity was used as the anode to compensate for the consumed nickel ions. As for the substrate, polished aluminum foil was utilized as the cathode. The reason for using the aluminum foil as the cathode is because the deposited nanocrystalline nickel can be easily separated from the foil by immersing it in a 50 g/l sodium hydroxide (NaOH) solution.

Table 1

Electrodeposition parameters

Sample #	Ni 01	Ni 02	Ni 03
$NiSO_4 \cdot 6H_2O$; g/l	350	350	350
$NiCl_2 \cdot 6H_2O$; g/l	45	45	45
H_3BO_3; g/l	37	37	37
Sodium lauryl sulphate (SLS); g/l	0.1	0.1	0.1
t_{on} (ms)	1	1	1
t_{off} (ms)	9	9	9
Peak current density ($mAcm^{-2}$)	450	750	1000

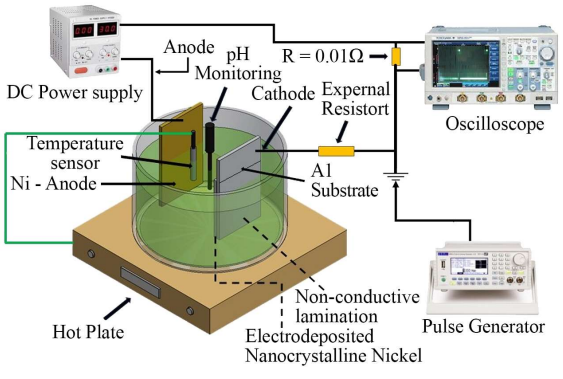

a

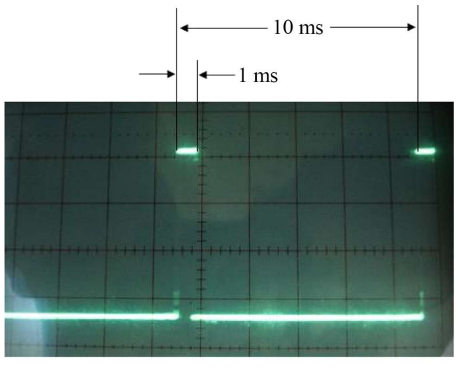

b

Fig. 1. Experimental apparatus for synthesis of electrodeposited nanocrystalline Nickel using single anode: *a* – circuit diagram; *b* – pulsed current of 1 ms on-time and 9 ms off-time with a peak current density of 1000 mA/cm^2

As shown in Fig. 1, *a*, deposition process was carried out on one substrate surface. While the other surface was laminated by a non-conductive material. A Pulsed generator was used to generate and control the on and off-time. Although it can generate an extra narrow pulse current, the apparatus was only able to generate on – off time in the range of milliseconds. Pulsed current monitoring was performed by an electroscope.

4. 2. Investigation of nanostructure

The two important methods performed for characterization of nanostructured electrodeposited nickel was investigated using XRD, TEM, and SEM to compare the following measurements. For TEM investigations, the grain size was derived from the linear intercept of grain, and XRD was used to determine grain sizes. Meanwhile, SEM was employed to study surface topologies.

During the XRD characterization, diffraction was carried out using CuK_α radiation with a wavelength of 0.1546 nm, which typically comprises $K_{\alpha 1}$ and a small portion of $K_{\alpha 2}$. In order to improve XRD analysis, $K_{\alpha 2}$ radiation needs to be extracted before any grain size calculation. Samples with a thickness of 70 to 100 μm were used in this experiment.

To determine the average grain size of electrodeposited nanocrystalline, the Scherrer equation can be used:

$$B_c = k\lambda\left(d\cos\theta\right)^{-1}. \quad (1)$$

In the above equation, k is a constant with a normal value of 0.9, λ represents the wavelength of the X-ray, and d denotes the grain size. Additionally, the parameter B_c refers to the full width at half peak maximum intensity (FWHM), which measures the width of an optical signal at half its maximum intensity. The last parameter was calculated by subtracting the observed experimental broadening (B_o) from the instrumental broadening (B_i) and strain broadening (B_s).

The crystalline broadening can be determined by:

$$B_r^2 = B_o^2 - B_i^2, \quad (2)$$

$$B_s = \eta\tan\theta, \quad (3)$$

$$B_c = B_r - B_s, \quad (4)$$

$$B_r\cos\theta = k\lambda d^{-1} + \eta\sin\theta. \quad (5)$$

In equation (2), B_r represents the FWHM after subtracting the instrumental broadening (B_i). The value of η can be obtained by plotting $B_r\cos q$ vs $\sin q$, where q represents the diffraction angle. The interception of the line in the $B_r\cos\theta$ axis gives the grain size, a method also employed by [16] as well as [22]. In addition to X-Ray Diffraction analysis, grain size measurements were also conducted using TEM by gauging the cross-section of grains in TEM images.

5. Result of the research on synthesis of nanocrystalline nickel and its nanoscale characterization

5. 1. Synthesis of electrodeposited nanocrystalline nickel

The initial experiment was conducted by investigating the ability of narrow pulse current of 0.05 ms on-time as well as 0.05 ms off-time. Current density of 100 mA/cm^2 was applied. A coarse structure was obtained as shown in Fig. 2.

The coarse grain size was believed due to inadequately off-time, so that deposition could not stop completely. Based on this finding, it was believed that longer off-time was needed. Further study found 9 ms off-time showed ideal off-time as shown in Fig. 1, *b*.

Further, three samples were produced using different peak current densities of 450, 750, and 1000 mA/cm^2 and identified as Ni 01, Ni 02, and Ni 03, respectively. Deposition processes were conducted in equal ion concentrations as well as the pulsed time. The thickness of deposited nickels was between 70 to 100 μm. Surface morphology investigated by Scanning Electron Microscopy of nickel deposits is shown in Fig. 3.

Typical pyramidal surfaces with different sizes are shown in all three deposits. The lower current density promoted a lower nucleation rate and a larger structure formed. As can be seen in Fig. 3, *a, b*, distance between pyramidal peaks were more than 2 μm. On the other hand, higher peak cur-

rent density promoted a higher nucleation rate. It appears a closer distance between pyramidal peaks which reflects finer structure. Another important data to note was the absence of porosities.

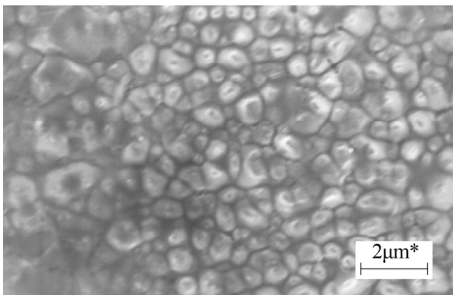

Fig. 2. Electrodeposited nickel synthesized using current density of 100 mA/cm^2 and 0.05 ms on-time and 0.05 off-time

5. 2. Nanoscale characterization

Nanoscale characterization was accomplished by XRD and TEM. Investigation using XRD showed the two important crystal orientations of (111) and (200) planes as shown in Fig. 4.

At high current density, it was observed a sifting of dominant crystal orientation from the (200) to the (111) plane. This alteration was attributed to the fact that massive atomic movements were only able to be accommodated at the densest crystal plane (111). Therefore, the atomic nuclei and growth in electrodeposited Ni 03 were following crystal planes of (111), (200), and (220). Lower current densities formed pyramidal structure as shown in Fig. 3 and confirmed with the model proposed by [21] that a lower peak current density leads to a lower nucleation rate. In addition, the absence of FWHM in the X-ray diffractogram in Fig. 4 also evidenced the existence of large grain sizes.

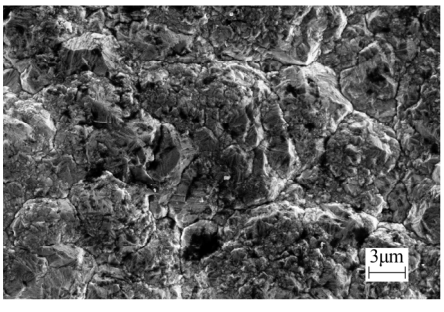

a

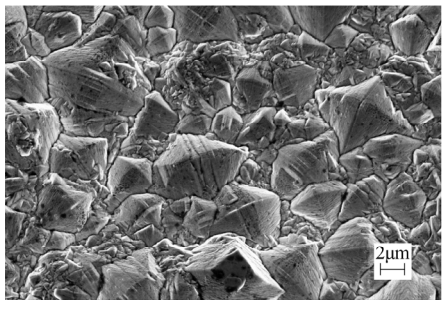

b

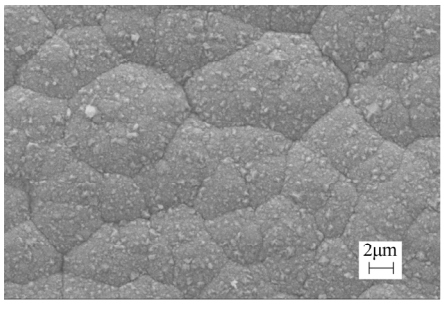

c

Fig. 3. Surface morphology of pulsed electrodeposition nickel: *a* — Ni 01; *b* — Ni 02; *c* — Ni 03

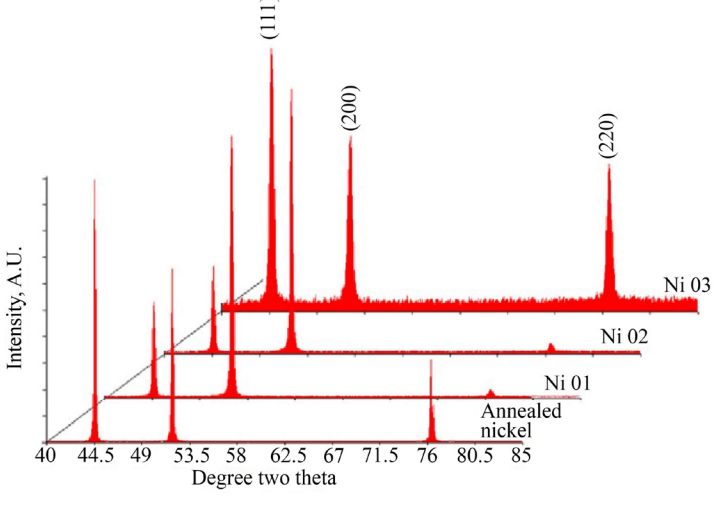

Fig. 4. The full width at half maximum peak intensity (FWHM) of Electrodeposited nickel N01, N02, and N03. As a comparison, X-ray Diffraction of annealed nickel with an average grain size of 93 mm

Structural investigation using TEM on sample Ni 02 also evidenced the presence of large grains that were not in the nanoscale range. It also confirmed by Selected Area Diffraction as shown in Fig. 5.

Based on the TEM image in Fig. 5, it was observed that the grain sizes are greater than 100 nm. It was also confirmed by Selected Area Diffraction. The next investigation was carried out on nanocrystalline nickel Ni 03 as shown in Fig. 6.

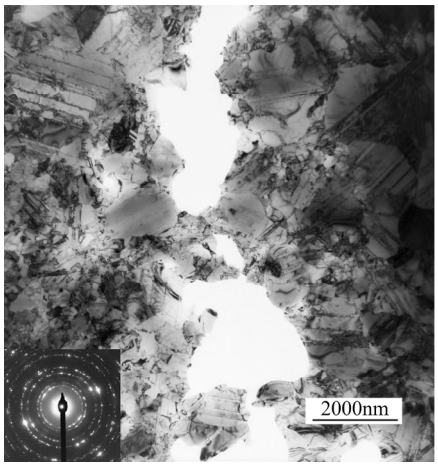

Fig. 5. Transmission electron microscopy investigation of deposited nickel Ni 02 and its selected area diffraction

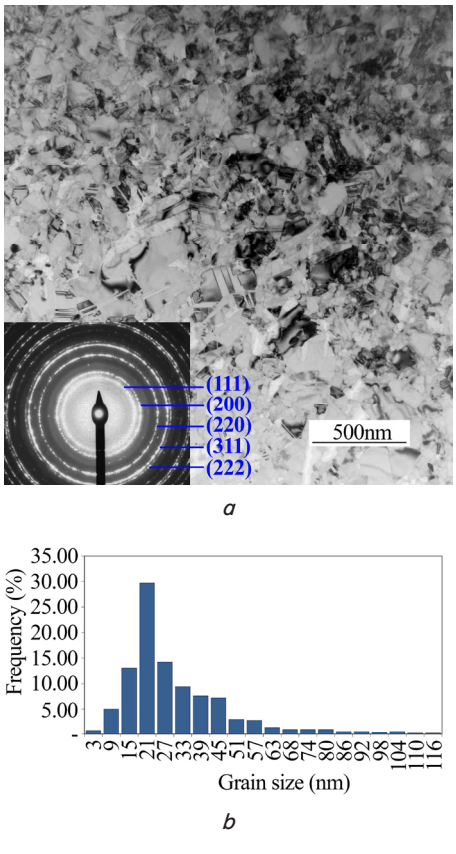

Fig. 6. Grain size determination of electrodeposited nanocrystalline nickel: *a* — Bright-field Transmission Electron Microscopy and its corresponding Selected Area Diffraction; *b* — grain size distribution of electrodeposited nanocrystalline nickel

Some grains have grain size more the 100 nm. The with the size of 21 nm represented the A careful scrutinizing on electrodeposited nanocrystalline Ni 03 showed an extraordinary data of its grain size. Small amount grain size of 3 nm was observed. This 3 nm nanocrystalline nickel was the smallest observed grain size. Whereas only largest quantity that can be measured. Meanwhile the average grain size of 25.4±3.4 nm was concluded.

6. Discussion of experimental on synthesis and its nanoscale characterization of electrodeposited nanocrystalline nickel

In the early stages of this experiment, electrodeposition was performed in an additive-free Watts bath. However, at the first run which was conducted with an extremely narrow pulse current of 0.05 on-time and off-time of 0.05 ms was unable to yield the nanoscale grain sizes as shown in Fig. 2. This limitation was believed due to an extremely short off-time that unable to stop the applied current perfectly. Consequently, a longer off times was employed. Based on that condition, systematic examination was performed to scrutiny the effective off time. It was concluded 9 ms off time gave an adequate duration to arrest the current completely as presented in Fig. 1, *b*. Therefore, a duty cycle with deposition times was decided to be set at 1ms and 9 ms of on-time and off-time respectively was applied.

Surface investigation on the first deposit which produced under current density of 450 mA/cm^2 exhibited large pyramidal structure. In addition, during examination using X-ray diffraction there was no peak broadening was observed. Further, no porosity was observed. Increasing the peak current densities to 750 mA/cm^2 and 1000 mA/cm^2 has led to a reduction of the deposited grain size and the absence of large pyramidal structures as shown in Fig. 3. This highlights the strong correlation between the deposited pyramidal size and peak current density. It also an evident a strong relation between peak current density and its nucleation rate. In a high current density, the distance between nuclei were closer compared to the lower one. Further, a horizontal growth (parallel to the substrate surface) of the structures were blocked when the grain met each other. A remarkable grain refinement was obtained by increasing the current density to 1000 mA/cm^2 as shown in Fig. 6. This finding agrees with [16]. Slight deferent was in measurement using Scherrer equation, in which, extraction of FWHF from electrodeposited nanocrystalline Ni-B which were deposited on to iron base substrate, whereas the present study used free standing pure nanocrystalline nickel. Important finding of elemental mapping conducted by [14] was existing of S in between nanocrystalline Ni, which is interpreted as element that arrest the nickel grain growth.

Regarding the measurement of grain size, two methods were employed for pulsed current electrodeposited nickel, namely XRD and TEM. The measurement based on TEM data was derived from a linear intercept of 498 grains bright field TEM conclude the grain size of 25.4±3.4 nm. Grain size distribution is shown in Fig. 5. In addition, Selected Area Diffraction (SAD) indicate the presence nanostructured nickel. The measured grains size was close to the size obtained from XRD data using the Scherrer

equation, namely 22 nm. The comparison of FWHM can be seen in Fig. 3, with significant broadening appearing in sample Ni 03, which was synthesized at the highest peak current density.

In term of crystallographic orientation, the electrodeposited nickel showed a different orientation. A strong intensity of (200) which is parallel to (100) was observed on the deposits that were synthesized with lower current density. A shifting of orientation from (200) to (111) was happen when deposit was produced using 1000mA/cm^2. This situation was believed to be related to different atomic density at different plane, in which higher adatoms were deposited in {111} plane.

7. Conclusions

1. Experiments have been conducted to investigate the formation of nanocrystalline nickel, with a focus on the effects of peak current density and nickel ion concentration on the grain size. The analysis involved the use of SEM, TEM, and XRD. The experimental parameters included peak current density of 450, 750, and 1000mA/cm^2, with on-time and off-time of 1ms and 9 ms, respectively, as well as equal Watts Bath. Notably, the peak current density played a significant role in the experiments. The highest value of 1000 mA/cm^2 was identified as the ideal current density for producing nanocrystalline nickel. Evidence was obtained to suggest that nanocrystalline metals can also be deposited in a Watts bath without any additive. Additionally, pulsed current was found to play a significant role in controlling deposition time and ensuring ionic movement. It was observed that higher current densities were required during electrodeposition in an additive-free Watts bath. The study also revealed a sifting in the dominant crystal orientation at low and high current densities from the (200) to (111) plane.

2. Measurement of grain size was accomplished using TEM, which showed a size of 25.4±3.4 nm, while the use of the Scherrer equation on XRD data concluded a grain size of 22 nm. Finally, it was recommended that the Scherrer equation needs to be employed for quick and accurate measuring of the grain size of nanocrystalline metals.

Conflicts of interest

The author declares that he has no conflicts of interest in relation to the current study, including financial, personal, authorship, or any other that could affect the study and the result reported in this paper.

Funding

The study was published without any financial support.

Data availability

All data are available in the main text of the manuscript.

Use of artificial intelligence

The authors confirm that they did not use artificial intelligence technologies when creating the current work.

References

1. Wasekar, N. P., Haridoss, P., Seshadri, S. K., Sundararajan, G. (2016). Influence of mode of electrodeposition, current density and saccharin on the microstructure and hardness of electrodeposited nanocrystalline nickel coatings. Surface and Coatings Technology, 291, 130–140. https://doi.org/10.1016/j.surfcoat.2016.02.024
2. Dong, Y., Yang, H., Zhang, L., Li, X., Ding, D., Wang, X. et al. (2020). Ultra-Uniform Nanocrystalline Materials via Two-Step Sintering. Advanced Functional Materials, 31 (1). https://doi.org/10.1002/adfm.202007750
3. Zhang, F., Yao, Z., Moliar, O., Tao, X., Yang, C. (2020). Nanocrystalline Ni coating prepared by a novel electrodeposition. Journal of Alloys and Compounds, 830, 153785. https://doi.org/10.1016/j.jallcom.2020.153785
4. Klapper, H. S., Zadorozne, N. S., Rebak, R. B. (2017). Localized Corrosion Characteristics of Nickel Alloys: A Review. Acta Metallurgica Sinica (English Letters), 30 (4), 296–305. https://doi.org/10.1007/s40195-017-0553-z
5. Wang, F., Li, L., Liu, J., Shu, Q. (2017). Research on tool wear of milling nickel-based superalloy in cryogenic. The International Journal of Advanced Manufacturing Technology, 91 (9-12), 3877–3886. https://doi.org/10.1007/s00170-017-0079-6
6. Zhou, X., Ouyang, C. (2017). Anodized porous titanium coated with Ni-CeO_2 deposits for enhancing surface toughness and wear resistance. Applied Surface Science, 405, 476–488. https://doi.org/10.1016/j.apsusc.2017.02.034
7. Merita, F., Umemoto, D., Yuasa, M., Miyamoto, H., Goto, T. (2018). Electrodeposition of nanocrystalline nickel embedded with inert nanoparticles formed via inverse hydrolysis. Applied Surface Science, 458, 612–618. https://doi.org/10.1016/j.apsusc.2018.07.123
8. Gu, C., Lian, J., He, J., Jiang, Z., Jiang, Q. (2006). High corrosion-resistance nanocrystalline Ni coating on AZ91D magnesium alloy. Surface and Coatings Technology, 200 (18-19), 5413–5418. https://doi.org/10.1016/j.surfcoat.2005.07.001
9. Zhou, X., Wu, F., Ouyang, C. (2017). Electroless Ni–P alloys on nanoporous ATO surface of Ti substrate. Journal of Materials Science, 53 (4), 2812–2829. https://doi.org/10.1007/s10853-017-1686-1
10. Fratesi, R., Ruffini, N., Malavolta, M., Bellezze, T. (2002). Contemporary use of Ni and Bi in hot-dip galvanizing. Surface and Coatings Technology, 157 (1), 34–39. https://doi.org/10.1016/s0257-8972(02)00137-8
11. Zeng, C., Tian, W., Liao, W. H., Hua, L. (2016). Microstructure and porosity evaluation in laser-cladding deposited Ni-based coatings. Surface and Coatings Technology, 294, 122–130. https://doi.org/10.1016/j.surfcoat.2016.03.083

12. Sadeghimeresht, E., Markocsan, N., Nylén, P., Björklund, S. (2016). Corrosion performance of bi-layer Ni/Cr_2C_3–NiCr HVAF thermal spray coating. Applied Surface Science, 369, 470–481. https://doi.org/10.1016/j.apsusc.2016.02.002
13. John, A., Saeed, A., Khan, Z. A. (2023). Influence of the Duty Cycle of Pulse Electrodeposition-Coated Ni-Al_2O_3 Nanocomposites on Surface Roughness Properties. Materials, 16 (6), 2192. https://doi.org/10.3390/ma16062192
14. Matsui, I., Watanabe, A., Takigawa, Y., Omura, N., Yamamoto, T. (2020). Microstructural heterogeneity in the electrodeposited Ni: insights from growth modes. Scientific Reports, 10 (1). https://doi.org/10.1038/s41598-020-62565-z
15. Watanabe, A., Yamamoto, T., Takigawa, Y. (2022). Tensile strength of nanocrystalline FeCoNi medium-entropy alloy fabricated using electrodeposition. Scientific Reports, 12 (1). https://doi.org/10.1038/s41598-022-16086-6
16. Cheng, A.-Y., Pu, N.-W., Liu, Y.-M., Hsieh, M.-S., Ger, M.-D. (2023). Evaluation of Ni–B alloy electroplated with different anionic groups. Journal of Materials Research and Technology, 27, 8360–8371. https://doi.org/10.1016/j.jmrt.2023.11.243
17. Rashidi, A. M., Amadeh, A. (2008). The effect of current density on the grain size of electrodeposited nanocrystalline nickel coatings. Surface and Coatings Technology, 202 (16), 3772–3776. https://doi.org/10.1016/j.surfcoat.2008.01.018
18. Moti, E., Shariat, M. H., Bahrololoom, M. E. (2008). Electrodeposition of nanocrystalline nickel by using rotating cylindrical electrodes. Materials Chemistry and Physics, 111 (2-3), 469–474. https://doi.org/10.1016/j.matchemphys.2008.04.051
19. Liu, H., Wang, H., Ying, W., Liu, W., Wang, Y., Li, Q. (2020). Influences of Duty Cycle and Pulse Frequency on Properties of Ni-SiC Nanocomposites fabricated by Pulse Electrodeposition. International Journal of Electrochemical Science, 15 (10), 10550–10569. https://doi.org/10.20964/2020.10.33
20. Lv, B., Hu, Z., Wang, X., Xu, B. (2015). Electrodeposition of nanocrystalline nickel assisted by flexible friction from an additive-free Watts bath. Surface and Coatings Technology, 270, 123–131. https://doi.org/10.1016/j.surfcoat.2015.03.012
21. Nayana, K. O., Ranganatha, S., Shubha, H. N., Pandurangappa, M. (2019). Effect of sodium lauryl sulphate on microstructure, corrosion resistance and microhardness of electrodeposition of Ni–Co3O4 composite coatings. Transactions of Nonferrous Metals Society of China, 29 (11), 2371–2383. https://doi.org/10.1016/s1003-6326(19)65143-5
22. Chauhan, M., Mohamed, F. A. (2006). Investigation of low temperature thermal stability in bulk nanocrystalline Ni. Materials Science and Engineering: A, 427 (1-2), 7–15. https://doi.org/10.1016/j.msea.2005.10.039